Photonic quantum information processing using the frequency continuous-variable of single photons

Nicolas Fabre[1] and Ulysse Chabaud[2]

[1]*Telecom Paris, Institut Polytechnique de Paris, 19 Place Marguerite Perey, 91120 Palaiseau, France*
[2]*DIENS, École Normale Supérieure, PSL University, CNRS, INRIA, 45 rue d'Ulm, Paris 75005, France*

(Dated: February 13, 2024)

The celebrated Hong–Ou–Mandel effect illustrates the richness of two-photon interferometry. In this work, we show that this richness extends to the realm of time-frequency interferometry. Taking advantage of the mathematical analogy which can be drawn between the frequency and quadrature degrees of freedom of light when there is a single photon in each auxiliary mode, we consider the equivalent of the Hong–Ou–Mandel effect in the frequency domain. In this setting, the n-Fock state becomes equivalent to a single-photon state with a spectral wave function given by the n^{th} Hermite–Gauss function and destructive interference corresponds to vanishing probability of detecting single photons with an order one Hermite–Gauss spectral profile. This intriguing analogy leads us to introduce an interferometric strategy using a frequency engineered two-photon state allowing to reach Heisenberg scaling for phase estimation, and to generalise the Gaussian Boson Sampling model to time-frequency degrees of freedom of single photons.

I. INTRODUCTION

Photonic quantum information processing is based on playing with fundamental bosonic properties of quantum states of light. The celebrated Hong–Ou–Mandel (HOM) bunching effect [1] provides one of the most basic but also striking examples of the nonclassical behaviour of photons. Boson Sampling [2], a computational generalisation of the HOM effect, has been introduced as a near-term candidate for harnessing the computational power of photonics. As such, its variant Gaussian Boson Sampling (GBS), defined in [3], led to the first attempts of demonstration of experimental quantum computational advantage using photonic platforms [4, 5].

The theoretical protocol for GBS involves the preparation of a multimode Gaussian quantum state and its measurement by a photon number-resolving detector in each mode. The probability of obtaining a given photon-number outcome is related to a combinatorial function known as the Hafnian, a quantity that is #P-hard to compute [6]. This approach directly utilizes entanglement, interference phenomena, and non-Gaussian operations to gain a potential quantum advantage over classical algorithms. The Hafnian is associated with various mathematical problems in graph theory, including graph isomorphism [7], the clique problem, perfect matching of undirected graphs, and finding dense subgraphs [8]. As a result, GBS has potential applications in quantum chemistry [9, 10] and quantum optimization [11], although the precise quantum advantage of GBS for specific computational tasks beyond sampling remains uncertain.

Many quantum optics platforms focus on degrees of freedom of quantum states of light such as polarization, spatial modes or time-bins, including the recent GBS experiments [4, 5]. However, quantum information can be also encoded using the time and frequency degrees of freedom of single photons, that are intrinsically continuous variables [12], but can be discretized into bins or modes. Recent advances have considerably improved the manipulation of the frequency (or spectral) degree of freedom of single photons: techniques that use pulse shapers and/or electro-optic modulators [13–18], or quadrature phase-shift keying modulators [19], allow for performing single photon operations, as well as two-photon operations [20]; other techniques for manipulating the time-frequency degree of freedom of photon pairs modify the temperature of the non-linear crystal at the generation stage [21, 22], by engineering the spatial distribution of the pump as in integrated circuits [23–25], in atomic cloud, or by engineering the spatial structure of the non-linear crystal [26–29].

In [30], a formalism to establish the mathematical correspondence between the quadrature and the frequency degrees of freedom considered as a continuous variable was established, based on the property that each auxiliary mode (other than the frequency) must be occupied by one single photon. This formalism opens new avenues for quantum information processing, enabling universal quantum computations by utilizing the frequency degree of freedom of single photons as a continuous-variable encoding of quantum information. Furthermore, it facilitates an understanding of the spectral (or temporal) width as a source of quantum noise in computing, as explored in earlier work [12, 31], and in recent quantum metrology protocols [32].

In this paper, based on this mathematical analogy between the quadrature and frequency continuous variables, we consider the equivalent of the HOM effect in the frequency domain of single photons. Following this analogy, N excitations of the electromagnetic field correspond to single-photon states with a Hermite–Gauss frequency spectrum of order N. The beam-splitter in the original HOM effect is replaced by a frequency beam-splitter which entangles the frequency of two single-photon states occupying two auxiliary modes [12, 30, 33], and performs a $\pi/4$ rotation of the joint spectral amplitude of two single photons. The final output is an intriguing frequency interference phenomena that suppress single photons in one frequency mode, similar to the destructive interference effect that leads to bunching in the HOM experiment. The proposed experiment in this paper can be seen as the continuous-variable counterpart of the one described in [34] using linear optics or with quantum frequency translation [35].

We then provide a first application of the frequency-based HOM effect in quantum metrology. Following the same analogy, we then define a quantum state composed of two-photon states with a spectrum that is the Hermite–Gauss function of or-

Quadratures variables	Time-frequency variables of single photons
$\hat{X}_a, \hat{P}_a, [\hat{X}_a, \hat{P}_a] = \hat{\mathbb{I}}$	$\hat{\omega}_a, \hat{t}_a, [\hat{\omega}_a, \hat{t}_a] = \hat{\mathbb{I}}$
$\hat{X}_a \lvert X\rangle_a = X \lvert X\rangle_a, \hat{P}_a \lvert P\rangle_a = P \lvert P\rangle_a$	$\hat{\omega}_a \lvert\omega\rangle_a = \omega \lvert\omega\rangle_a, \hat{t}_a \lvert t\rangle_a = t \lvert t\rangle_a$
Vacuum state	Single photon with a Gaussian spectrum
N-Fock state	Single photon with a Hermite–Gauss spectral function of order N
$\hat{U}_{BS} \lvert X_s, X_i\rangle_{ab} = \left\lvert \frac{X_s+X_i}{\sqrt{2}}, \frac{X_s-X_i}{\sqrt{2}} \right\rangle_{ab}$	$\hat{U} \lvert\omega_s, \omega_i\rangle_{ab} = \left\lvert \frac{\omega_s+\omega_i}{\sqrt{2}}, \frac{\omega_s-\omega_i}{\sqrt{2}} \right\rangle_{ab}$

TABLE I. Analogy between the quadratures and the time-frequency degrees of freedom. The analogy holds as soon as the auxiliary modes a, b are populated by one single photon. The name "frequency beam-splitter" comes from the mathematical equivalence to the standard beam-splitter operation in the quadrature domain.

der N (see [36, 37] and develop the strategy developed adapted from [38] for reaching the Heisenberg limit for phase estimation. This avoids the use of large entangled quantum states of many photons for reaching the Heisenberg scaling, similarly to strategies developed using the orbital angular momentum of one single photon [39].

Finally, our mathematical correspondence finds application in quantum computing through the novel concept of GBS generalized in the continuous time-frequency variables of single photons. In this protocol, we start from single photons with a Gaussian spectrum (that are mathematically equivalent to squeezed states), that enter into an interferometer performing time-frequency Gaussian operations. The output state is a time-frequency Gaussian state whose chronocyclic Wigner distribution [12, 40, 41] is Gaussian. The final step involves single photon mode-resolved detection, which is projection onto a spectral Hermite–Gauss basis, coupled with measurements employing single-photon detectors, thereby simulating the equivalent of photon number-resolving detection. A given configuration is given here as the simultaneous measurement of N single-photon states with Hermite–Gauss mode spectrum $n_1, ...n_N$. In time-frequency GBS, a configuration involves the measurement of specific single-photon states, each associated with its respective Hermite–Gauss mode spectrum, in contrast to Boson sampling where configurations are defined by the detection of single photon states, irrespective of their degrees of freedom structure. The importance of this result is that combining time-frequency Gottesman–Kitaev–Preskill states [12, 31, 42, 43] with a time-frequency GBS interferometer provides an architecture for realizing a fault-tolerant quantum computer, similar to what has been proposed in the quadrature domain [44].

The rest of the paper is organized as follows. In Sec. II, we develop the essential tools for understanding the formalism describing the frequency degree of freedom of single photons. In Sec. III, we discuss the continuous-variable frequency HOM effect by using the mathematical analogy between the quadrature and the frequency degree of freedom. Following this analogy in Sec. IV, we then develop a quantum metrology protocol relying on a two-photon probe whose frequency spectrum is engineered so that to achieve Heisenberg scaling for phase estimation. Finally in Sec. V, we translate the GBS model to the frequency degree of freedom of single photons.

II. FREQUENCY-BASED QUANTUM INFORMATION PROCESSING

We recall the formalism of a single photon with a continuous-variable frequency degree of freedom. A single photon with a frequency ω in the spatial mode (or any other auxiliary mode) a is denoted $\hat{a}^\dagger(\omega) \lvert\Omega\rangle_a$, where $\lvert\Omega\rangle_a$ is the vacuum state. The Fourier transform of a creation operator in the frequency domain correspond to a creation operator in the temporal domain. We introduce the frequency and time operators as:

$$\hat{\omega}_a = \int_{\mathbb{R}} d\omega\, \omega\, \hat{a}^\dagger(\omega)\hat{a}(\omega), \tag{1}$$

$$\hat{t}_a = \int_{\mathbb{R}} dt\, t\, \hat{a}^\dagger(t)\hat{a}(t). \tag{2}$$

Although frequencies and times are nonnegative, the integration is over $\mathbb{R}$ without loss of generality: in practice wave functions are localized far away from the origin. If the auxiliary mode is populated by a single photon, the frequency and time operator verify the Heisenberg–Weyl canonical commutation relation [30]:

$$[\hat{\omega}_a, \hat{t}_a] = \hat{\mathbb{I}}. \tag{3}$$

Therefore, we must have in each spatial mode only one single photon for the mathematical analogy between the quadrature and frequency variables to hold. Equipped with this mathematical analogy, a single photon with a Gaussian frequency spectrum becomes mathematically analogous to the vacuum state in the quadrature domain:

$$\lvert 0\rangle_a \equiv \frac{1}{(\pi\sigma^2)^{1/4}} \int_{\mathbb{R}} d\omega e^{-\omega^2/2\sigma^2} \lvert\omega\rangle_a , \tag{4}$$

where σ is the frequency width of the Gaussian spectrum. A single photon spectrum is centered around a certain value that we will omit, which depends on the physical system producing such a single photon. Such a state would be actually the equivalent of a coherent state in the quadrature domain, but as we will set the central frequency to zero, the state becomes equivalent to the vacuum. Then, the n^{th} Fock state is in this encoding a single photon with a Hermite–Gauss frequency spectrum corresponding to the wave function [45]:

$$\lvert n\rangle_a \equiv \frac{1}{(\pi\sigma^2)^{1/4}} \int_{\mathbb{R}} d\omega \frac{1}{\sqrt{2^n n!}} H_n(\omega/\sigma) e^{-\omega^2/2\sigma^2} \lvert\omega\rangle_a , \tag{5}$$

where for instance $H_0(x) = 1, H_1(x) = 2x$ and $H_2(x) = 4x^2-2$. We can check that $\langle n|m\rangle = \delta_{nm}$. Projecting the state into $\langle n|$ reads as first performing a frequency filtering operation with the Hermite–Gauss filter $H_n(\omega/\sigma)e^{-\omega^2/2\sigma^2}/\sqrt{2^n n!}$ and then a non-resolved frequency detection (that is modeled by an integration over the frequency variable). The projector defined as $\hat{\Pi}(n) = |n\rangle\langle n|$ could be implemented experimentally by using a spatial light modulator for shaping the spectral distribution of the single photon. The projection of a single photon into the Fock-like basis is therefore: $\langle\hat{\Pi}(n)\rangle = |\langle n|\psi\rangle|^2$, which corresponds to a frequency filtering in the Hermite–Gauss basis followed by non-resolved frequency detection. From the mathematical correspondence between the quadrature and the time-frequency, we can perform the correspondence between the number of photons (Fock state) into a spatial mode, and the Hermite–Gauss spectral mode of a single photon. A similar mapping from Fock states to Hermite–Gauss modes of the *spatial* degree of freedom of single photons was previously proposed [46], together with proposal for the violation of a Bell inequality.

In the frequency domain, the equivalent of the beam-splitter is the frequency beam-splitter [12, 30, 33] which performs the operation:

$$\hat{U}\,|\omega_s,\omega_i\rangle_{ab} = \left|\frac{\omega_s+\omega_i}{\sqrt{2}},\frac{\omega_s-\omega_i}{\sqrt{2}}\right\rangle_{ab}. \tag{6}$$

Such an operation performs a $\pi/4$ rotation of the joint spectral amplitude of two single photons, leading them to frequency entanglement if the initial joint spectral amplitude was separable (see Fig. II). Besides, each input and output modes (a, b) are occupied by one and only one single photon. Akin to the beam-splitter in the quadrature domain (see Fig. I), this is a Gaussian operation for the frequency continuous variable [45, 47]. A similar operation has been achieved experimentally by using a quantum dot embedded into a waveguide where the efficiency of one process is of 99% [48] (see also [49] for further theoretical study).

Due to possible confusion in the denomination or experimental apparatus, we should emphasize that in [34, 50], they define an analogous beam-splitter where the two spatial modes of the standard beam-splitter are now two frequency modes. We want also to emphasize that the frequency beam-splitter is not a frequency-dependent beam-splitter [51, 52], since such a device acts on the quadrature as a standard beam-splitter but with frequency-dependent reflection coefficient.

Another time-frequency gate that will be important in this paper is the fractional Fourier transform [45] that can be cast as:

$$\hat{F}(\phi) = \exp(i\phi(\hat{\omega}^2+\hat{t}^2-\hat{\mathbb{I}})), \tag{7}$$

and which has been demonstrated experimentally in [16]. Note that we have employed dimensionless units for the frequency and time operators, as it was done in the transversal position-momentum of single photons [53]. The fractional Fourier transform in the frequency domain is equivalent to the phase-shift operation $e^{i\phi\hat{b}^\dagger\hat{b}}$ in the quadrature domain.

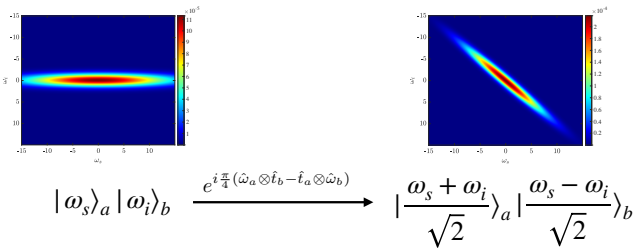

FIG. 1. Two initially separable single photons have Gaussian frequency spectrums with different widths, and their joint spectral intensity is represented on the left. After the action of a frequency beam-splitter, the photon pair is now entangled, and the frequency beam-splitter acts as a $\pi/4$ rotation of the spectrum. The equivalent process in the quadrature domain is to start with two single-mode squeezed states which become an entangled two-mode squeezed state after a standard beam-splitter operation.

III. HOM EFFECT IN THE FREQUENCY DOMAIN OF SINGLE PHOTONS

Let us assume that we start with two separable single photon in spatial paths a, b that possess the same Hermite–Gauss spectrum $|\psi\rangle = |1,1\rangle_{a,b} := |1\rangle_a \otimes |1\rangle_b$ (see Eq. (5)), and let us proceed to the equivalent of the HOM experiment: the state $|\psi\rangle$ is sent into a frequency beam-splitter (see Eq. (6)). After such an operation, we remain in the single-photon subspace for each output spatial mode. The output wave function after the frequency beam-splitter is given by:

$$\hat{U}\,|\psi\rangle = \frac{1}{(\pi\sigma^2)^{1/2}}\iint d\omega d\omega' \frac{1}{2}H_1\left(\frac{\omega}{\sigma}\right)H_1\left(\frac{\omega'}{\sigma}\right) \times e^{-\omega^2/2\sigma^2}e^{-\omega'^2/2\sigma^2}\left|\frac{\omega+\omega'}{\sqrt{2}},\frac{\omega-\omega'}{\sqrt{2}}\right\rangle_{ab}. \tag{8}$$

We perform a change of variable to obtain:

$$\hat{U}\,|\psi\rangle = \frac{1}{(\pi\sigma^2)^{1/2}}\iint d\omega d\omega' \frac{1}{2}H_1\left(\frac{\omega+\omega'}{\sqrt{2}\sigma}\right)H_1\left(\frac{\omega-\omega'}{\sqrt{2}\sigma}\right) \times e^{-(\omega+\omega')^2/4\sigma^2}e^{-(\omega-\omega')^2/4\sigma^2}\,|\omega,\omega'\rangle_{ab}. \tag{9}$$

In the standard HOM interference, the output wave function written with quadrature variables is not often employed, however, in the particle-number representation the output state is given by

$$\frac{1}{\sqrt{2}}(|2,0\rangle_{ab}-|0,2\rangle_{ab}+|1,1\rangle_{ab}-|1,1\rangle_{ab}) = \frac{1}{\sqrt{2}}(|2,0\rangle_{ab}-|0,2\rangle_{ab}), \tag{10}$$

which clarifies the origin of the destructive interference between coincidence events.

In comparison, in the frequency domain, we obtain a destructive interference between different frequency modes, i.e., the equivalent of a "frequency bunching" effect. Indeed, from Eq. (8), we have $H_1(\frac{\omega+\omega'}{\sqrt{2}\sigma})H_1(\frac{\omega-\omega'}{\sqrt{2}\sigma}) = \frac{\omega^2}{\sigma^2}-\frac{\omega'^2}{\sigma^2}$ which corresponds directly to the two bunched terms, and we do not

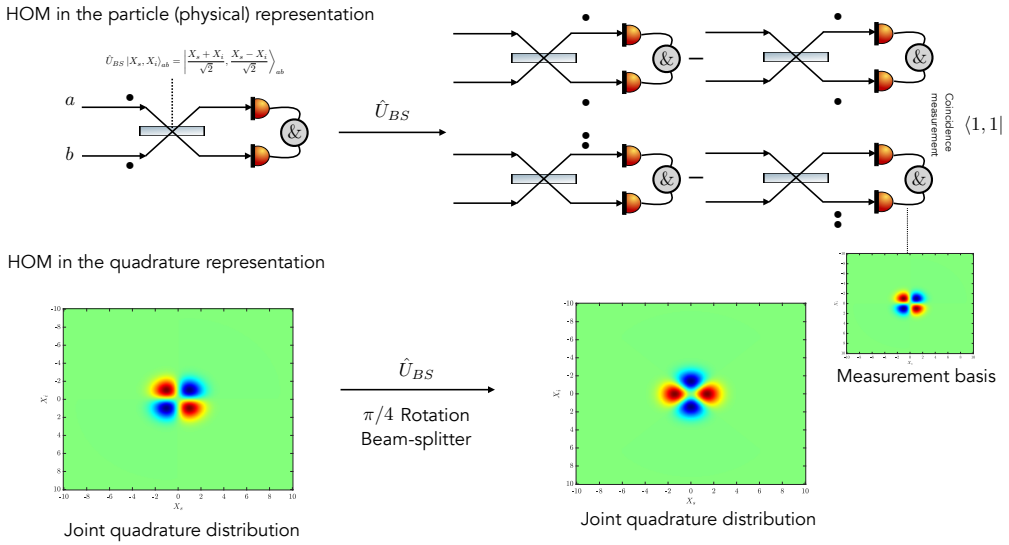

FIG. 2. Standard HOM experiment, analysed both in the particle representation and by representing the joint quadrature distribution at each step. Two indistinguishable single photons are combined on a balanced beam-splitter that is modeled by the unitary operation $\hat{U}$. Coincidence measurement is performed in both arms of the interferometer. In the quadrature representation, the state that was initially separable becomes entangled after the beam-splitter. As the input and the output are orthogonal (it corresponds to a rotation of the joint quadrature distribution), thus the corresponding measured probability is zero.

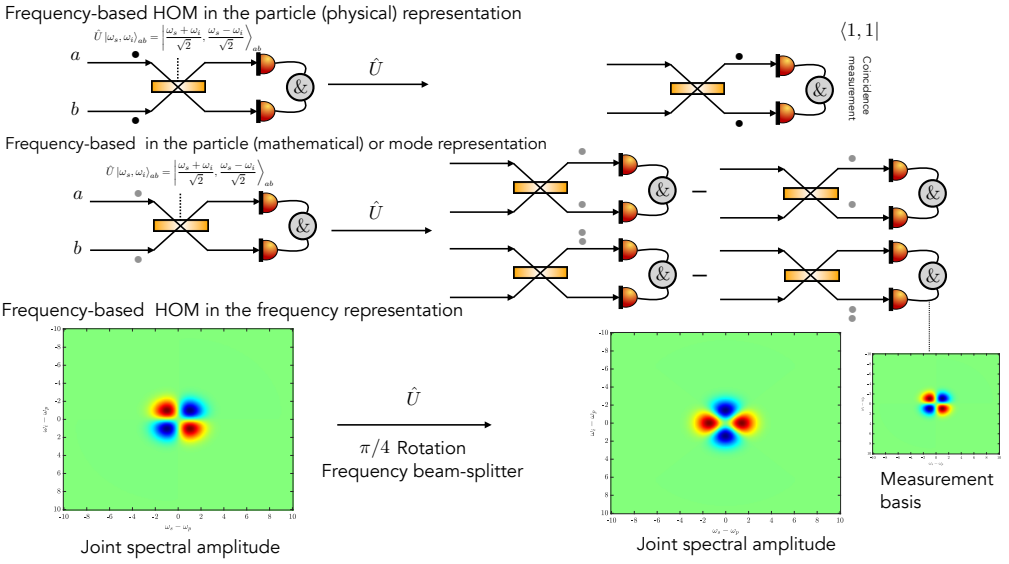

FIG. 3. Frequency-based HOM experiment using the spectral degree of freedom of single photons. We start from two separable single photon with a Hermite–Gauss spectrum or order one, that become frequency entangled after the frequency beam-splitter operation. We obtain an equivalent destructive interference which does not affect the total particle number (that stays fixed during the frequency beam-splitter operation) but the spectral degree of freedom of each single photon. Each path (a, b) is always occupied by one single photon, as represented in the particle (physical) representation. In the particle (mathematical) or mode representation, black dots are not single photon, but instead represent the Hermite–Gauss mode labeling of the spectral degrees of freedom, from which we understand the destructive interference between different spectral contributions.

get any order one polynomial. Projecting the state into the equivalent of coincidences $\langle 1,1|$ (which is a photon number-resolving detection in the quadrature domain) corresponds to applying first a spectral filtering corresponding to the first order Hermite–Gauss function and then applying a non-frequency resolved detection [54, 55]. It corresponds to a mode-resolved detection for only the mode 1. The probability of detecting the photon pair in coincidence in the frequency modes 1, 1 is then:

$$\left|{}_{ab}\langle 1,1|\,\hat{U}\,|\psi\rangle\right|^2 = |\,\langle 1,1|\,\frac{1}{\sqrt{2}}(|2,0\rangle_{ab} - |0,2\rangle_{ab})|^2, \quad (11)$$

which is zero. Thus, we have obtained a non-trivial destructive frequency interference between two single photons having an order 1 Hermite–Gauss frequency spectrum, which is the analogue of the HOM effect in the frequency domain.

In Fig. 2 and Fig. 3, we have represented the continuous-variable quadrature (resp. frequency) states before and after the beam-splitter (resp. frequency beam-splitter). The beam-splitter has the effect of performing a rotation of the joint spectrum, leading to an entangled state in the quadrature and the frequency domains, respectively.

IV. PHASE ESTIMATION AT THE HEISENBERG LIMIT USING TWO-PHOTON INTERFEROMETRY

In this section, we provide a two-photon quantum state and a new measurement strategy reaching Heisenberg scaling for the estimation of a phase parameter ϕ that is the analogous in the frequency domain to the one in the quadrature [38], which is difficult to implement experimentally when N is the number of excitation of the electromagnetic field.

We start with the two-photon state $|N,N\rangle_{ab}$, which corresponds to a separable two-photon state with Hermite–Gauss spectrums of order N, and is therefore mathematically analogous to a twin-Fock state [38]. Then, this two-photon state enters in the interferometer described in Fig. 4, which contains a frequency beam-splitter followed by a fractional Fourier transform in the frequency domain (see Eq. (7)), and finally by another frequency beam-splitter. This is a non-linear interferometer, as frequency beam-splitters require light-matter interaction for their implementation. The detection is composed of two single-photon detectors that are resolved in frequency modes. In other words, this is a mode-resolved detector that is in perfect analogy with photon-number resolved detector. The probability of measuring the frequency modes $N-q$ and $N+q$ at the spatial ports a and b is given by:

$$P(q|\phi) = \left|\langle N-q, N+q|\,\hat{V}_{ab}\,|N,N\rangle\right|^2, \quad (12)$$

where $\hat{V}_{ab} = \exp(-\phi/2(\hat{\omega}_a\hat{\imath}_b - \hat{\omega}_b\hat{\imath}_a))$ (see Sec. II for the definition of the time and frequency operators). The probability is found to be for $q \ll N$ [38]:

$$P(q|\phi) = J_q^2(\phi N), \quad (13)$$

where J_q is a Bessel function of the first kind. The precision over the phase parameter that can be reached with such an interferometer is bounded by the Cramér–Rao bound:

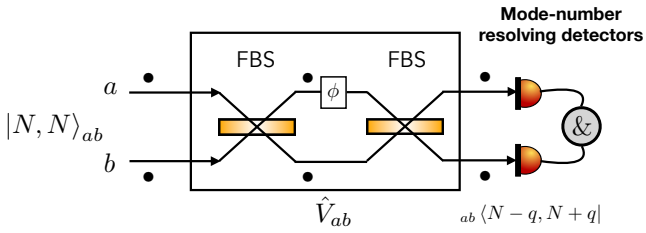

FIG. 4. Interferometry at the Heisenberg limit for phase estimation with a two-photon state. The protocol starts with a separable two-photon state whose spectrum is a Hermite–Gauss function of order N. The two photon state becomes entangled by a first frequency beam-splitter (FBS), and crosses the sample that induces a frequency shift. A measurement in an entangled basis is then performed, that is composed of frequency beam-splitter and a mode-resolved detector.

$$\Delta\phi \geq \frac{1}{\sqrt{\nu F(\phi)}}, \quad (14)$$

where ν is the number of repetitions of the experiment and $F(\phi)$ is the Fisher information that can be written in our case:

$$F(\phi) = \sum_q \frac{\left(J_q^2(\phi N) - J_{q-1}^2(\phi N)\right)^2}{J_q^2(\phi N)}, \quad (15)$$

where the sum over q is taken until 30. Numerical analysis shows that the Fisher information scales as $F(\phi) \sim N^2$ for large N, so that the sensitivity for the phase estimation is $\Delta\phi \sim 1/N$, which corresponds to Heisenberg scaling. In this protocol, we only use two photons, which is economical in terms of resources for reaching Heisenberg scaling compared to phase estimation protocols using N-photon states. This is an example of spectral engineering of photon pairs that is employed for reaching better resolution over the measurement of a parameter as it was done in [56]. Apart from the fractional Fourier transform and the mode-resolved measurement, the main challenge in this protocol lies in performing the frequency-entangling operation.

Note that experimentally, reaching the Heisenberg scaling with a twin-Fock state when N is the number of atoms in a Bose-Einstein condensate is easier to implement experimentally [57], while this is difficult to achieve experimentally when N denotes the number of photons.

V. GAUSSIAN BOSON SAMPLING IN THE FREQUENCY DOMAIN OF SINGLE PHOTONS

A. Description of the protocol

With such equivalence between quadrature and frequency degrees of freedom of single photons, we obtain straightforwardly the equivalent of the GBS in the frequency domain

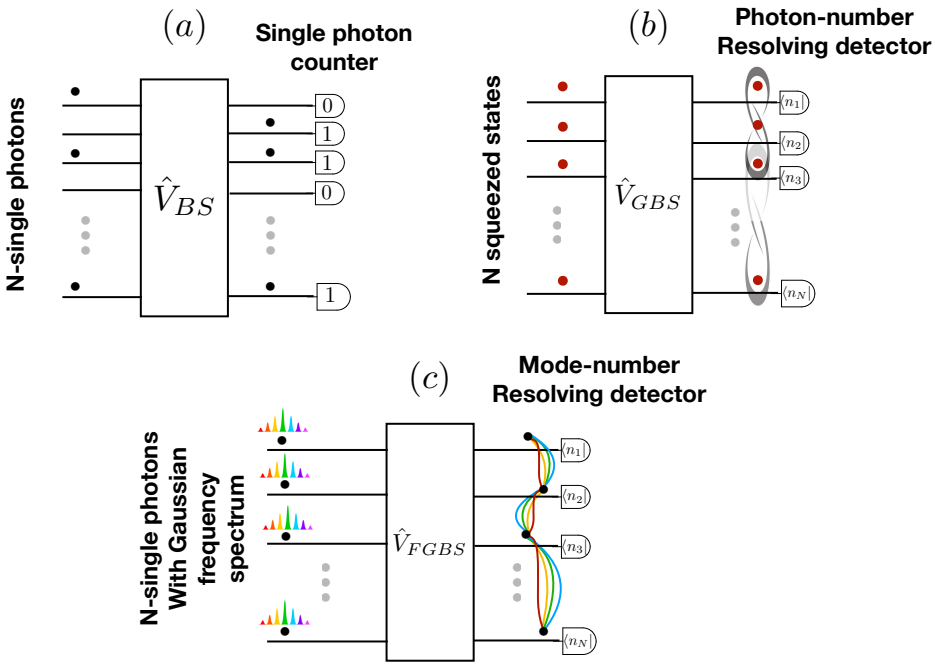

FIG. 5. (a) Boson Sampling, where each black dot corresponds to a single photon occupying one single spatial mode. The output state is an entangled state of a presence/absence of single photon into N spatial modes. (b) GBS, where each red dot corresponds to a single-mode squeezed state. The output state after the Gaussian operation is a multimode entangled Gaussian state that is then measured with N photon number-resolving detectors. (c) FGBS experiment, where each black dot supplemented by a frequency comb indicated one single photon with a Gaussian *continuous* spectral structure. The output state after the time-frequency interferometer is a multimode (spatial for instance) time-frequency entangled Gaussian state (schematized with colored lines) that is then measured with frequency mode resolved detectors.

of single photons, which we call Frequency-based Gaussian Boson Sampling (FGBS).

We start from the mathematical analogue of N squeezed states which are N single photons with a Gaussian spectrum. These states undergo Gaussian time-frequency operations. The time-frequency Gaussian state is a state whose chronocyclic Wigner distribution is Gaussian and characterized by the covariance matrix Σ (see [30, 45] for more details). These time-frequency Gaussian operations can be achieved with linear and non-linear optics (for generating entanglement with the frequency beam-splitter) [30]. Measurements are performed with a set of single-photon detectors that have been frequency filtered. This allows for a mode-number resolved detection as described in the previous section. The probability distribution of detecting a total of N photons (one photon at each auxiliary mode output) in the spectral configuration $\vec{n} = (n_1, ..., n_N)$, where n_i labels the frequency modes in the output i, is [3]:

$$P(\vec{n}) = |\Sigma_Q|^{-1/2} \frac{\mathrm{Haf}(A_{\vec{n}})}{\prod_{i=1}^{N} n_i!} \tag{16}$$

where $\Sigma_Q = \Sigma + \mathbb{I}_{2N}$ and $A = \begin{pmatrix} 0 & \mathbb{I} \\ \mathbb{I} & 0 \end{pmatrix} (\mathbb{I} + (\Sigma + \mathbb{I}/2)^{-1})$, with $A_{\vec{n}}$ the $2n \times 2n$ submatrix of A obtained by repeating n_i times its rows and columns i and $N + i$, where $n = \sum_i n_i$ is the sum of the labels of the detected modes. The function Haf is the Hafnian: for a $2n \times 2n$ matrix B,

$$\mathrm{Haf}(B) = \frac{1}{n! 2^n} \sum_{\sigma \in S_{2n}} B_{\sigma(1)\sigma(2)} \dots B_{\sigma(2n-1)\sigma(2n)}, \tag{17}$$

where the sum is over the permutations of $\{1, \dots, 2n\}$.

Therefore, the FGBS is a non-linear optics scheme to generate samples extracted from a mode distribution generated by a time-frequency light source at the output of a multimode interferometer. The hardness of the classical simulation of this sampling task is preserved in noisy experimental condition if the level of photon losses and temporal and frequency broadening (mathematically similar to loss in GBS) are limited.

Using single photons and their continuous-variables spectral distribution in FGBS leads us to a model that "mixes" both features of Boson sampling and GBS. In Fig. 5, we have represented the three types of bosonic samplers based on Boson sampling, GBS and FGBS. The Boson Sampling protocol involves N indistinguishable single photons entering an N-mode interferometer. Phase interference determines the exit point of each single photon from the interferometer. If the interferometer is sufficiently deep, each output mode contains only a single

photon. A configuration is identified by the detector that registers a click. GBS, as previously discussed, is mathematically equivalent to FGBS.

B. Experimental considerations

Experimentally, implementing the FGBS algorithm could involve utilizing an integrated circuit designed to take as input n single photon states with a Gaussian spectrum. It is worth noting that currently, single photon sources with a frequency Gaussian spectrum are not readily available; typically, they exhibit a Lorentzian spectrum, as demonstrated in [58].

However, heralded single-photon sources offer a workaround, as they can have a Gaussian spectrum when the initial photon pair also exhibits one. This can be achieved through techniques such as engineering the spatial poling of the non-linear crystal [59] or using an integrated AlGaAs circuit [60]. In contrast to Boson Sampling, where the performance is limited by the challenge of creating exactly identical single-photon sources, our protocol is not constrained by the need for identical photon pair sources. This flexibility arises from our ability to initiate the process with different time-frequency squeezed states.

Similar to the preceding sections, a fundamental element for a multimode interferometer achieving large frequency entanglement among single photons is the frequency beam-splitter [48, 49]. Current implementations are near-deterministic, so cascading multiple frequency beam-splitters provides a credible pathway towards the generation of large frequency-entangled states of single photons. Detection involves the use of superconducting nanowire single-photon detectors (SNSPDs) that are resolved in frequency mode number. A challenge arising from the cryogenic operational conditions of SNSPDs involves integrating the single-photon source, the interferometer, and the detection onto a single chip. Such an integration was recently experimentally accomplished in [61].

VI. CONCLUSION

In this paper, we have used the correspondence between the quadrature and the frequency degrees of freedom of single photons to design an analogue of the HOM effect in the frequency domain. In this scheme, there is a non-trivial destructive effect between different components of the frequency spectrum of two single photons, leading to a suppression of the part of the spectrum with first order Hermite–Gauss function. We have employed a graphical representation that allows us to understand this destructive interference effect for any type of continuous variables, instead of using the standard particle-number representation.

We have discussed a direct application of the correspondence to a quantum metrology protocol that can reach Heisenberg scaling for phase estimation using two photons and frequency mode resolving detection.

Finally, we have discussed the equivalent of GBS in the frequency domain of single photons, established thanks to the mathematical correspondence between the position-momentum quadratures of the electromagnetic field into a single mode and the time-frequency variables of single photons.

We expect this work to motivate further development of spectral interferometry experiments. As a perspective, we note that our results are also valid for other types of continuous variables, such as the position and momentum of a nanomechanical resonator, or the transversal position and momentum of single photons [62].

ACKNOWLEDGMENTS

N. Fabre acknowledges fruitful discussion with Olivier Pfister and Pérola Milman. U. Chabaud acknowledges interesting discussions with Jack G. Davis.

[1] C.-K. Hong, Z.-Y. Ou, and L. Mandel, Phys. Rev. Lett **59**, 2044 (1987).
[2] S. Aaronson and A. Arkhipov, Theory of Comput. **9**, 143 (2013).
[3] C. Hamilton, R. Kruse, L. Sansoni, S. Barkhofen, C. Silberhorn, and I. Jex, Physical Review Letters **119** (2016).
[4] H.-S. Zhong, L.-C. Peng, Y. Li, Y. Hu, W. Li, J. Qin, D. Wu, W. Zhang, H. Li, L. Zhang, Z. Wang, L. You, X. Jiang, L. Li, N.-L. Liu, J. P. Dowling, C.-Y. Lu, and J.-W. Pan, Science Bulletin **64**, 511 (2019).
[5] L. S. Madsen, F. Laudenbach, M. F. Askarani, F. Rortais, T. Vincent, J. F. F. Bulmer, F. M. Miatto, L. Neuhaus, L. G. Helt, M. J. Collins, A. E. Lita, T. Gerrits, S. W. Nam, V. D. Vaidya, M. Menotti, I. Dhand, Z. Vernon, N. Quesada, and J. Lavoie, Nature **606**, 75 (2022).
[6] L. Valiant, Theoretical Computer Science **8**, 189 (1979).
[7] K. Brádler, S. Friedland, J. Izaac, N. Killoran, and D. Su, Special Matrices **9**, 166 (2021).
[8] J. M. Arrazola and T. R. Bromley, Phys. Rev. Lett. **121**, 030503 (2018).
[9] L. Banchi, M. Fingerhuth, T. Babej, C. Ing, and J. M. Arrazola, Science Advances **6**, eaax1950 (2020).
[10] J. Huh, G. G. Guerreschi, B. Peropadre, J. R. McClean, and A. Aspuru-Guzik, Nature Photonics **9**, 615 (2015).
[11] J. M. Arrazola, T. R. Bromley, and P. Rebentrost, Phys. Rev. A **98**, 012322 (2018).
[12] N. Fabre, G. Maltese, F. Appas, S. Felicetti, A. Ketterer, A. Keller, T. Coudreau, F. Baboux, M. I. Amanti, S. Ducci, and P. Milman, Phys. Rev. A **102**, 012607 (2020).
[13] J. M. Lukens and P. Lougovski, Optica **4**, 8 (2017).
[14] A. Henry, R. Raghunathan, G. Ricard, B. Lefaucher, F. Miatto, N. Belabas, I. Zaquine, and R. Alléaume, Phys. Rev. A **107**, 062610 (2023).
[15] S. Kurzyna, M. Jastrzębski, N. Fabre, W. Wasilewski, M. Lipka, and M. Parniak, Opt. Express **30**, 39826 (2022).

[16] B. Niewelt, M. Jastrzębski, S. Kurzyna, J. Nowosielski, W. Wasilewski, M. Mazelanik, and M. Parniak, Phys. Rev. Lett. **130**, 240801 (2023).

[17] P. Imany, J. A. Jaramillo-Villegas, M. S. Alshaykh, J. M. Lukens, O. D. Odele, A. J. Moore, D. E. Leaird, M. Qi, and A. M. Weiner, npj Quantum Inf **5**, 59 (2019).

[18] M. Kues, C. Reimer, J. M. Lukens, W. J. Munro, A. M. Weiner, D. J. Moss, and R. Morandotti, **13**, 170 (2019).

[19] C. Chen, J. E. Heyes, J. H. Shapiro, and F. N. C. Wong, Sci Rep **11**, 300 (2021).

[20] H.-H. Lu, J. M. Lukens, B. P. Williams, P. Imany, N. A. Peters, A. M. Weiner, and P. Lougovski, npj Quantum Information **5** (2019).

[21] Y. Chen, M. Fink, F. Steinlechner, J. P. Torres, and R. Ursin, npj Quantum Information **5** (2019).

[22] R.-B. Jin, R. Shiina, and R. Shimizu, Optics Express **26**, 21153 (2018), 1805.00148.

[23] S. Francesconi, F. Baboux, A. Raymond, N. Fabre, G. Boucher, A. Lemaître, P. Milman, M. I. Amanti, and S. Ducci, Optica **7**, 316 (2020).

[24] G. Maltese, M. I. Amanti, F. Appas, G. Sinnl, A. Lemaître, P. Milman, F. Baboux, and S. Ducci, npj Quantum Inf **6**, 13 (2020).

[25] S. Francesconi, A. Raymond, N. Fabre, A. Lemaître, M. I. Amanti, P. Milman, F. Baboux, and S. Ducci, ACS Photonics **8**, 2764 (2021).

[26] A. Dosseva, L. Cincio, and A. M. Branczyk, Phys. Rev. A **93**, 013801 (2016), 1410.7714 [quant-ph].

[27] R.-B. Jin, R. Shimizu, M. Fujiwara, M. Takeoka, R. Wakabayashi, T. Yamashita, S. Miki, H. Terai, T. Gerrits, and M. Sasaki, Quantum Sci. Technol. **1**, 015004 (2016), 1603.07887.

[28] K.-H. Luo, V. Ansari, M. Massaro, M. Santandrea, C. Eigner, R. Ricken, H. Herrmann, and C. Silberhorn, Opt. Express **28**, 3215 (2020).

[29] X. Gao, Y. Zhang, A. D'Errico, F. Hufnagel, K. Heshami, and E. Karimi, Opt. Express **30**, 21276 (2022), 2203.06260 [quant-ph].

[30] N. Fabre, A. Keller, and P. Milman, Physical Review A **105** (2022), 10.1103/physreva.105.052429.

[31] N. Fabre, Applied Sciences **13**, 9462 (2023).

[32] E. Descamps, N. Fabre, A. Keller, and P. Milman, Phys. Rev. Lett. **131**, 030801 (2023).

[33] N. Fabre, Journal of Modern Optics **69**, 653 (2022), https://doi.org/10.1080/09500340.2022.2073613.

[34] P. Imany, O. D. Odele, M. S. Alshaykh, H.-H. Lu, D. E. Leaird, and A. M. Weiner, Optics Letters **43**, 2760 (2018).

[35] H. J. McGuinness, M. G. Raymer, and C. J. McKinstrie, Optics Express **19**, 17876 (2011).

[36] P. Kok, H. Lee, and J. P. Dowling, Phys. Rev. A **65**, 052104 (2002).

[37] J. P. Dowling, Contemporary Physics **49**, 125 (2008).

[38] M. J. Holland and K. Burnett, Phys. Rev. Lett. **71**, 1355 (1993).

[39] V. D'Ambrosio, N. Spagnolo, L. Del Re, S. Slussarenko, Y. Li, L. C. Kwek, L. Marrucci, S. P. Walborn, L. Aolita, and F. Sciarrino, Nature Communications **4**, 2432 (2013).

[40] C. Dorrer and I. A. Walmsley, EURASIP Journal on Advances in Signal Processing **2005** (2005), 10.1155/ASP.2005.1541.

[41] B. Brecht and C. Silberhorn, Phys. Rev. A **87** (2013).

[42] T. Yamazaki, T. Arizono, T. Kobayashi, R. Ikuta, and T. Yamamoto, Phys. Rev. Lett. **130**, 200602 (2023).

[43] E. Descamps, A. Keller, and P. Milman, (2023), 2310.12618 [quant-ph].

[44] J. E. Bourassa, R. N. Alexander, M. Vasmer, A. Patil, I. Tzitrin, T. Matsuura, D. Su, B. Q. Baragiola, S. Guha, G. Dauphinais, K. K. Sabapathy, N. C. Menicucci, and I. Dhand, Quantum **5**, 392 (2021), 2010.02905 [quant-ph].

[45] N. Fabre, *Quantum information in time-frequency continuous variables*, Ph.D. thesis, Université de Paris (2020).

[46] A. F. Abouraddy, T. Yarnall, B. E. A. Saleh, and M. C. Teich, Physical Review A **75** (2007).

[47] P. M. Eloi Descamps, Arne Keller, Phys. Rev. A **108** (2023).

[48] H. L. Jeannic, A. Tiranov, J. Carolan, T. Ramos, Y. Wang, M. H. Appel, S. Scholz, A. D. Wieck, A. Ludwig, N. Rotenberg, L. Midolo, J. J. García-Ripoll, A. S. Sørensen, and P. Lodahl, Nature Physics **18**, 1191 (2022).

[49] U. Alushi, T. Ramos, J. J. García-Ripoll, R. Di Candia, and S. Felicetti, PRX Quantum **4**, 030326 (2023).

[50] N. S. Jones and T. M. Stace, Phys. Rev. A **73**, 033813 (2006).

[51] D. N. Makarov, E. S. Gusarevich, A. A. Goshev, K. A. Makarova, S. N. Kapustin, A. A. Kharlamova, and Y. V. Tsykareva, Sci Rep **11** (2021).

[52] D. N. Makarov, "Theory for the beam splitter in quantum optics: quantum entanglement of photons and their statistics, HOM effect," (2022), 2211.03359 [physics, physics:quant-ph].

[53] D. S. Tasca, R. M. Gomes, F. Toscano, P. H. Souto Ribeiro, and S. P. Walborn, Phys. Rev. A **83**, 052325 (2011).

[54] T. Legero, T. Wilk, A. Kuhn, and G. Rempe (Academic Press, 2006) pp. 253–289.

[55] N. Fabre, J. Belhassen, A. Minneci, S. Felicetti, A. Keller, M. I. Amanti, F. Baboux, T. Coudreau, S. Ducci, and P. Milman, Phys. Rev. A **102**, 023710 (2020), 2003.11486 [quant-ph].

[56] N. Fabre and S. Felicetti, Physical Review A **104**, 022208 (2021).

[57] L. Pezzé, A. Smerzi, G. P. Berman, A. R. Bishop, and L. A. Collins, Phys. Rev. A **74**, 033610 (2006).

[58] N. Somaschi, V. Giesz, L. De Santis, J. C. Loredo, M. P. Almeida, G. Hornecker, S. L. Portalupi, T. Grange, C. Antón, J. Demory, C. Gómez, I. Sagnes, N. D. Lanzillotti-Kimura, A. Lemaítre, A. Auffeves, A. G. White, L. Lanco, and P. Senellart, Nature Photonics **10**, 340 (2016).

[59] A. Dosseva, L. Cincio, and A. M. Brańczyk, Phys. Rev. A **93**, 013801 (2016).

[60] J. Belhassen, F. Baboux, Q. Yao, M. Amanti, I. Favero, A. Lemaître, W. S. Kolthammer, I. A. Walmsley, and S. Ducci, Applied Physics Letters **112**, 071105 (2018).

[61] N. A. Lange, J. P. Höpker, R. Ricken, V. Quiring, C. Eigner, C. Silberhorn, and T. J. Bartley, Optica **9**, 108 (2022).

[62] D. S. Tasca, R. M. Gomes, F. Toscano, P. H. S. Ribeiro, and S. P. Walborn, Physical Review A **83**, 052325 (2011).